International Journal of High Speed Electronics and Systems, Vol. 12, No. 3 (2002) 925–937

ERRATA

SPECIAL ISSUE: FRONTIERS IN ELECTRONICS: FUTURE CHIPS

(edited by Y. S. PARK, M. S. SHUR and W. TANG)
[International Journal of High Speed Electronics and Systems
Vol. 12, No. 2 (2002), 491–500]

The following paper is the updated version of the one published in the above issue:

THz DETECTION BY RESONANT 2-D PLASMONS IN FIELD EFFECT DEVICES

X. G. PERALTA and S. J. ALLEN
Center for Terahertz Science and Technology, University of California, Santa Barbara, California 93106, USA

M. C. WANKE, N. E. HARFF, M. P. LILLY, J. A. SIMMONS and J. L. RENO
Sandia National Laboratories, Albuquerque, New Mexico 87185, USA

P. J. BURKE and J. P. EISENSTEIN
Department of Physics, California Institute of Technology, Pasadena, California 91125, USA

W. KNAP[a], Y. DENG, S. RUMYANTSEV[b], J.-Q. LÜ and M. S. SHUR
Dept. of ECSE and Center for Broadband Data Transport Science and Technology, Rensselaer Polytechnic Institute, Troy, NY 12180, USA

We demonstrate resonant detection of terahertz radiation by two-dimensional plasma waves in two field effect devices: a commercial field effect transistor (FET) and a double quantum well field effect transistor with a periodic grating gate. In both devices, the standing 2-D plasmon is tuned to the frequency of the THz radiation by varying the gate bias. The double quantum well field effect transistors exhibits a rich photoconductive response corresponding to spatial harmonics of the standing 2-D plasmons under the metal part of the periodic gate.

[a] Also with GES CNRS-Universite Montpellier2 34950 Montpellier, France
[b] On leave from the Ioffe Institute of Russian Academy of Sciences, 194021 St-Petersburg, Russia

Introduction

The terahertz part of the electromagnetic spectrum lies in a gap in solid-state technology between semiconductor electronics and photonics. Tunable solid-state sources and detectors are key elements for the development of this part of the spectrum. There are a large variety of terahertz incoherent and coherent detectors - hot-electron bolometers[1,2,3], composite bolometers, superconducting-insulator-superconducting (S-I-S) junctions[4,5], pyroelectric detectors[6], Schottky diodes[7,8] and photoconductive detectors[9]. Tunability has been demonstrated in magnetic field tuned photoconductivity from hydrogenic donors in lightly doped GaAs[10] and InSb.[11] Here we explore the potential of developing detectors tuned by plasmon resonances in field effect structures.[12,13] Tuning the detector response by gate voltage is more attractive for applications than tuning with a magnetic field.

In this paper, we describe two different approaches. First, we report on a field effect transistor (FET) THz detector, where the standing 2-D plasmon is tuned to the frequency of the THz radiation by varying the gate bias. Second, we fabricate double quantum well field effect transistors with a periodic grating gate, which exhibit a rich spectrum corresponding to standing 2-D plasmons under the metal part of the periodic gate. This FET structure can also be tuned to the THz frequency by applying a gate bias. Both sets of experiments demonstrate the feasibility of tunable resonant detection of THz radiation by plasmons in a gated two dimensional electron gas.

I. *Plasma wave detectors in a gated FET*

There exists a great interest in new solid state devices that could detect and emit terahertz radiation in a selective and tunable way. The difficulty in detecting and generating terahertz radiation using solid state devices is related to two factors: i) the transit times in the devices are typically much longer than the period of the terahertz oscillations and ii) the quanta of terahertz radiation are much smaller than room or even liquid nitrogen thermal energy. However, plasma waves in a gated two dimensional electron gas can propagate with much larger velocity than the electron drift velocity and their excitation is not linked to any type of electronic transition. Hence, they can be excited even at elevated temperatures[14]. Allen et al. observed infrared absorption[15], and Tsui et al. reported weak infrared emission related to plasma waves in silicon inversion layers[16]. Burke et al. showed that the impedance of a high mobility transistor exhibits maxima at the fundamental plasma frequency and its harmonics[17].

The theory in Ref. [12] predicted that a constant drain-to-source voltage might be induced by electromagnetic radiation coupled into the channel of a field-effect transistor (FET). In a high mobility channel, this constant drain-to-source voltage should have a resonant dependence on the radiation frequency, with the resonant frequency being proportional to the square root of the surface carrier density and inversely proportional to the gate length. With carrier densities on the order of $10^{12}cm^{-2}$ and the gate length dimensions below 1 μm the FET plasma frequency can reach the THz range[13]. The carrier density can be tuned by the gate-to-source voltage. This implies that a FET may be used as a resonant tunable detector of THz radiation.

Plasma waves that may propagate in a FET channel have a linear dispersion law, $\omega(k) = sk$. Here s is the plasma wave velocity that depends on carrier density, and k is the wave vector. The velocity of the plasma waves, s, is typically on the order of 10^8 cm/s,

which is much larger than the drift velocity of the two-dimensional (2D) electrons in the FET channel. This is why the propagation of plasma waves can be used for new regimes of FET operation, with a much higher frequency than for conventional, transit-time limited devices. In a FET with a given length L the values of plasma frequencies are discrete and given by[13] $\omega_N = \omega_0 (1+2N)$, where $\omega_0 = \pi s/2L$, and $N = 0, 1, 2, \ldots$.

A FET, biased by the gate-to-source voltage and subjected to electromagnetic radiation, can develop a constant drain-to-source voltage, which has a resonant dependence on the radiation frequency, $f=\omega/2\pi$, with the maxima at the plasma oscillation frequencies $f_N=\omega_N/2\pi$. The plasma wave velocity depends on the carrier density in the channel n, and the gate to channel capacitance per unit area C, as $s=(e^2n/mC)^{1/2}$, where e is the electron charge and m is the electron effective mass. In the gradual channel approximation, the carrier density in the channel is related to the gate voltage as $n=CU_0/e$. U_0 is the gate to channel voltage swing defined as $U_0=U_g - U_{th}$, where U_g is the gate voltage and U_{th} is the threshold voltage. In this case, the fundamental plasma frequency can be expressed by an approximate relation $f_o=\omega_0/2\pi=(eU_0/m)^{1/2}/4L$. This relation leads to two important consequences: i) a sufficiently short (sub-micron) FET can operate as a THz detector and ii) the frequency of this detector can be tuned by the gate voltage.

The dimensionless parameter determining the detector behavior is $\omega\tau$, where $\omega=2\pi f$, f is the radiation frequency and τ is the momentum scattering time. Two opposite cases ($\omega\tau >> 1$ and $\omega\tau << 1$) have to be considered. When $\omega\tau >> 1$, the FET can operate as a resonant detector. When $\omega\tau << 1$, the plasma oscillations are overdamped and the detector response is a smooth function of ω as well as of the gate voltage (broadband detector)[18]. There have been a few experimental observations of the non-resonant detection[19]. However, the final experimental confirmation of the possibility of resonant detection of THz radiation and the theoretical description of the nonresonant signal close to the threshold voltage were open questions for a long time.

The FETs used in the experiments were commercial GaAs/AlGaAs field effect transistors (Fujitsu FHR20X) with the gate length L = 0.15 μm. They were removed from packages and mounted on a quartz plate in order to avoid any parasitic interference and reflections.

The photo-response measurements were performed with 200 GHz and 600 GHz radiation systems based on a 100 GHz Gunn diode with a frequency doubler (for the 200 GHz system) or doubler and tripler (for the 600 GHz system). The maximum output power was about 3 mW for the 200 GHz system and 0.3 mW for the 600 GHz system, respectively. Attenuators were used in order to limit the power at the focused spot to about 0.1 mW in order to avoid heating effects. A waveguide finished with a cylindrical cone was connected to the output of the Gunn diode to out-couple the radiation. The radiation beam was then focused by a parabolic mirror and led through the cryostat window to the sample, which was placed on a quartz substrate glued to the cold finger of the closed cycle cryostat. The radiation beam diameter at the sample holder was ~1mm – a dimension that was much larger than the device size. No special coupling antennas were used and the terahertz radiation was coupled to the device through metallization pads. In each measurement, we tested a few parabolic mirror orientations and a few incident angles in order to verify possible interference effects. We found that different beam geometry/incidence angles changed only the amplitude of the signal and not its spectral shape.

The radiation intensity was modulated with a mechanical chopper (30–300 Hz range) and the open-circuit source drain voltage was measured by a voltage preamplifier (1 MΩ input resistance) followed by a lock-in amplifier. A regulated temperature system allowed temperature stabilization to within 1K over the range from 8-300 K.

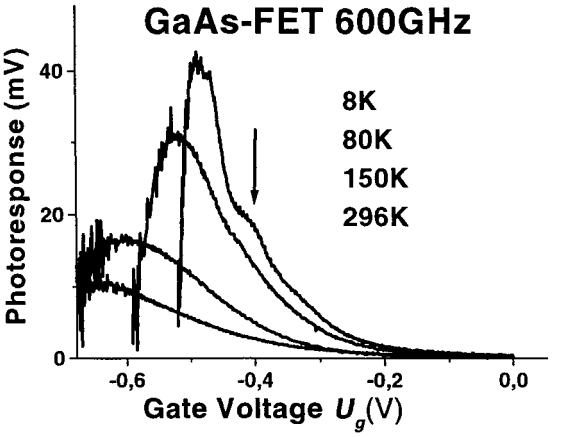

Figure 1. Measured photoresponse of the GaAs/AlGaAs 0.15μm FET for the 600GHz radiation. Radiation induced source - drain voltage as a function of the gate voltage Ug is shown for temperatures 8K, 80K, 150K, 296K. The arrow marks the maximum corresponding to the resonant detection observed at the lowest temperature 8K.[21]

In Fig.1, we show a few examples of typical experimental data. The drain–source voltage photoinduced by the 600 GHz radiation in the GaAs/AlGaAs FET, is shown as a function of the gate voltage, U_g. At the lowest temperature (8K), one can see a resonant feature in the response (marked by an arrow in Fig.1) that is superimposed on the broad background. It is due to resonant detection of 600GHz radiation. The resonant response appears at the lowest temperatures, since, at these temperatures, the electron scattering time increases and we reach $\omega_0\tau=1$ - the condition for resonant detection. The resonant detection was reported recently in (see Ref. 20) and will be described in more detail later.

Let us first concentrate on the nonresonant part of the signal. For relatively large positive gate voltage swings, U_0, the detector response falls off as $1/U_0$. For negative values of U_0 (U_g smaller than the threshold voltage), the experimentally observed response decreases, so that the response always reaches a maximum value close to the FET threshold. This maximum changes its position and amplitude with the temperature but not with the frequency of the radiation.

In order to understand the origin of the maximum one has to take into account the leakage current from the metal gate to the 2D electron gas in the channel. Well above threshold, the gate leakage is small compared to the current in the channel and does not affect the response of the detector. However, for negative values of U_0, when electron concentration in the FET channel becomes exponentially small, the leakage current plays an important role and should be taken into account.

A new theoretical approach that takes into account the gate leakage current has been recently developed (see Ref. 21). Below we will discuss its main results.

The general equation for the electron concentration in the FET channel is given by

$$n = n^* \ln\left[1+\exp\left(\frac{eU_0}{\eta k_B T}\right)\right]. \tag{1}$$

Here $n^* = \frac{C\eta k_B T}{e^2}$, C is the gate capacitance per unit area and η is the ideality factor.

The response of the FET can be expressed as

$$\Delta u = \frac{eu_a{}^2}{(4\eta k_B T)} \frac{1}{\left(1+\exp\left(-\frac{eU_0}{\eta k_B T}\right)\right)\left(1+\kappa\exp\left(-\frac{eU_0}{\eta k_B T}\right)\right)\ln\left(1+\exp\left(\frac{eU_0}{\eta k_B T}\right)\right)} \tag{2}$$

where $\kappa = \frac{j_0 L^2 me}{2C\tau\eta^2 k_B^2 T^2}$ is the dimensionless parameter characterizing the leakage current j_0, and u_a is the ac gate to drain voltage induced by external illumination. Results of the calculation of the detector response are shown in Fig.2.

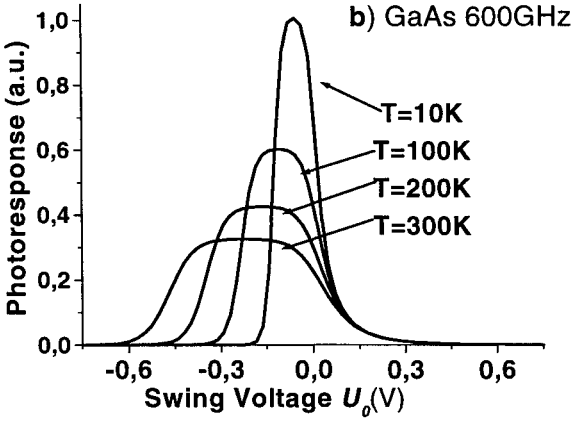

Figure 2. Photoresponse of the GaAs/AlGaAs FET at 600GHz - as calculated according Eq.22. response for a leakage current density ($j_0 = 1.3*10^3 A/m^2$) at four different temperatures η and κ- values: (T=10K, η=15, κ=9.0x10^{-5}), (T=100K, η=2.5, κ=3.2x10^{-5}), (T=200K, η=1.75, κ=1.7x10^{-5}) and (T=300K, η=1.5, κ=10^{-5}).[21]

The temperature dependence of the photoresponse shown in Fig.2 represents a typical device behavior. One can see that the temperature evolution of the width and the amplitude of the photoresponse curves shown in Fig.2 qualitatively agree with the measured curves shown in Fig.1. (The photoresponse results in Fig.1 are shown as a function of the gate voltage U_g). At low temperatures a well defined maximum is

observed and at high temperatures a broad maximum, or rather a step-like behavior near the device threshold voltage is observed. Generally, the shape of the photoresponse curve defined by Eq.2 is a function of two main parameters: $\eta k_B T$ that governs the carrier density in the subthreshold region (see Eq.1) and κ, which is a dimensionless parameter related to the leakage current.

The maximum value of photoresponse depends only on $\eta k_B T$. The width and the position of the maximum depend both on $\eta k_B T$ and κ. For small κ, the photoresponse has a plateau (or step like) behaviour near the threshold. For higher values of κ, the photoresponse has a well defined maximum. These rules, although approximate, allow us to understand the photoresponse in most experimental situations. More detailed discussion of nonresonant detection of THz radiation by submicron FET's can be find in Ref. 21.

As can be seen in Fig.1 at the lowest temperatures the resonant-like maximum is superimposed on the background. A region of the resonance response is shown in more detail in Fig. 3. At the lowest temperatures (below 30 K) a well reproducible maximum - superimposed on the background was observed. The inset of Fig.3a shows the shape of the maximum after subtraction of the nonresonant background signal.

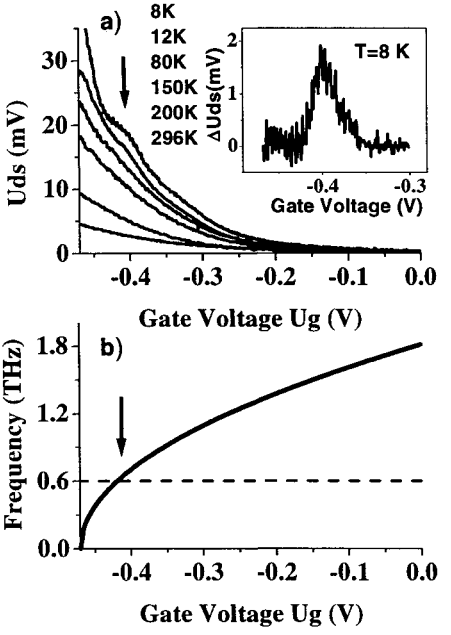

Figure 3. a)Experimental drain response U_{ds} for different temperatures. The results for temperatures 296K (the lowest curve), 200K, 150K, 80K, 12K and 8K (the highest curve) are shown. Inset shows the resonant signal ΔU_{ds} at 8 K obtained after subtraction of the $1/U_0$ like background from the experimental result. b) Resonant plasma frequency as a function of the gate voltage. The vertical arrow shows the cross point with 600GHz horizontal line – the voltage of the expected resonant detection.[20]

In Fig.3b, we plotted the plasma frequency versus gate voltage dependence for U_{th} =0.47. As can be seen, the resonant frequency of the transistor decreases with applied gate voltage from its maximum value ~1.8THz (at zero gate bias) to zero, which is reached when the gate voltage is equal to the threshold voltage. The horizontal line in figure 3b corresponds to 600GHz, which is the measurement frequency used in this work. One can see that the expected position of the resonance (marked by an arrow) is close to the one observed in the experiment. In order to get a more quantitative description of the results we use the following expressions for the drain response derived in Ref. 13:

$$U_{ds} = \frac{1}{4}\frac{U_a^2}{U_0} f(\omega) \tag{3}$$

where

$$f(\omega) = 1 + \beta - \frac{1 + \beta\cos(2k_0' L)}{\sinh^2(k_0'' L) + \cos^2(k_0' L)} \quad , \beta = \frac{2\omega\tau}{\sqrt{1+(\omega\tau)^2}},$$

$$k_0' = \frac{\omega}{s}(1/\beta + 1/2)^{1/2} \text{ and } k_0'' = \frac{\omega}{s}(1/\beta - 1/2)^{1/2}.$$

Here U_a is the ac gate to drain voltage induced by external illumination. Using Eq. (3), we calculated the expected detector response using the device parameters determined from the I-V and magnetoresistance measurements for different temperatures. The results are shown in Fig.4. As can be seen from a comparison of Fig.3a and Fig.4 a good overall agreement of measured and calculated spectra was obtained. The temperature evolution of the background, as well as the position and the width of the resonant signal seen in the experiment (Fig.3a) are well reproduced in the calculated spectra (Fig.4).

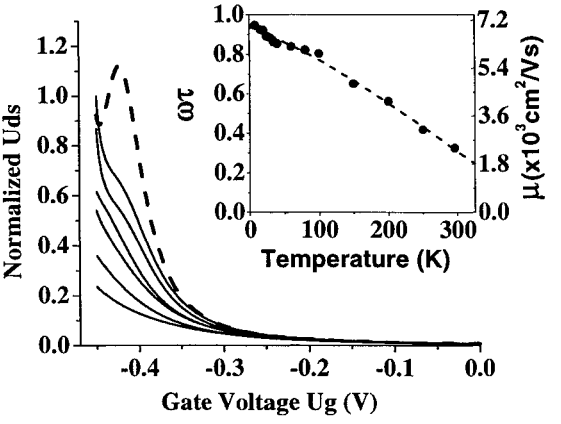

Figure 4. Drain-source voltage U_{ds} for different temperatures calculated according to Eq.1. The results are normalized to the U_{ds} value at U_g=0.47V for temperature 8K. The results for temperatures 296K (the lowest solid curve), 200K, 150K, 80K, 12K and 8K (the highest solid curve) are shown. The expected increase of the detector response when $\omega\tau$ slightly increases to 1.5 is shown by a dashed line. The inset shows the change of electron mobility μ and $\omega\tau$ for 600GHz with decreasing temperature, the dashed line is a guide for the eye.[21]

In order to understand the temperature evolution of the spectra one has to consider the change of the $\omega\tau$ parameter. The measured mobility μ versus temperature dependence is plotted in the inset in Fig.4. As can be seen (right hand scale), the mobility increases with decreasing temperature. The momentum scattering time was calculated as $\tau=\mu m^*/e$. On the left hand side scale of the inset, we show the value of $\omega\tau$ for the frequency of 600 GHz. One can see that at temperatures above 50K $\omega\tau<<1$. At temperatures below 30K, one can approach the condition of resonant detection ($\omega\tau = 1$) . This explains why at higher temperatures only the $1/U_0$ –like non-resonant background is observed but at low temperatures, a resonant feature is superimposed on this background. This behavior is well seen in the experimental data (Fig. 3a) and in the theoretical calculations (Fig.2). The value of the $\omega\tau$ parameter also determines the sensitivity of the detector. (The expected increase of the detector response when $\omega\tau$ slightly increases to 1.5 is shown by a dashed line in Fig.4). One expects a very high sensitivity of such detectors for high mobility GaAs FETs[13].

II. *Resonant plasmons in grating gated double quantum well FET*

Here we explore the terahertz response of grating gated double quantum well field effect devices. The devices are fabricated from modulation doped GaAs/AlGaAs double quantum well heterostructures grown on a semi-insulating GaAs substrate by molecular beam epitaxy. The quantum wells are 200Å wide and are separated by a 70Å barrier. The nominal electron densities in the quantum wells are $n_{upper}=1.7x10^{11}cm^{-2}$ and $n_{lower}=2.57x10^{11}$ cm^{-2}: the 4.2K mobility is ~$1.7x10^6$ cm^2/Vs. A 2x2mm mesa is defined by wet chemical etching and the ohmic contacts to both quantum wells are formed by evaporating and annealing NiAuGe over the edge and side of the mesa forming source and drain. A 700Å thick TiAu grating gate (with no metallization between the grating fingers) is evaporated with the lines of the grating parallel to the ohmic contacts, perpendicular to the current flow. Devices with grating periods of 4 and 8 μm were tested (In both cases half of the period was metal the other half open.). The grating has three different functions: 1) modulation of the electron density in the quantum wells under the metallized part, 2) selection of the wavevectors of the excited plasmon and 3) production of both normal and transverse THz electric fields inside the sample.

The terahertz sources used are the free-electron lasers at UCSB, which cover a frequency range between 120 GHz and 4.8 THz, but the experiments were performed between 570 and 660 GHz. To measure the terahertz photoresponse, the samples are wire bonded and mounted on a fiberglass chip carrier inside a variable temperature cryostat. Radiation is focused onto the sample by means of an off-axis parabolic mirror. A constant source-drain current of 100μA is applied and we study the photoconductive response of the double quantum wells as a function of gate voltage, terahertz frequency and temperature.[22] Part of the terahertz radiation is split off by means of a mylar beam splitter to the reference detector and is focused, using an off-axis parabolic mirror, onto a fast pyroelectric detector that acts as a reference. In order to account for pulse-to-pulse variations in the output power of the free-electron laser and be able to compare results for different frequencies, the photoconductive signal was normalized by dividing it by the signal from the reference pyroelectric detector therefore all the data presented has been normalized.

Fig. 5 shows the grating gate (4μm period) voltage dependent photoresponse at T=25K for different incident radiation frequencies. For 570GHz there is a resonance in the photoresponse around V_{gate}= −1.6V. This resonant peak moves to lower negative gate voltage, higher electron density, as we increase the frequency of the incident radiation. This is typical of plasmons, which invariably exhibit an increasing frequency with increasing electron density. [23,24,25] The response was a linear function of terahertz power and source drain current, indicating a photoconductive response. The radiation is polarized perpendicular to the lines of the grating gate.

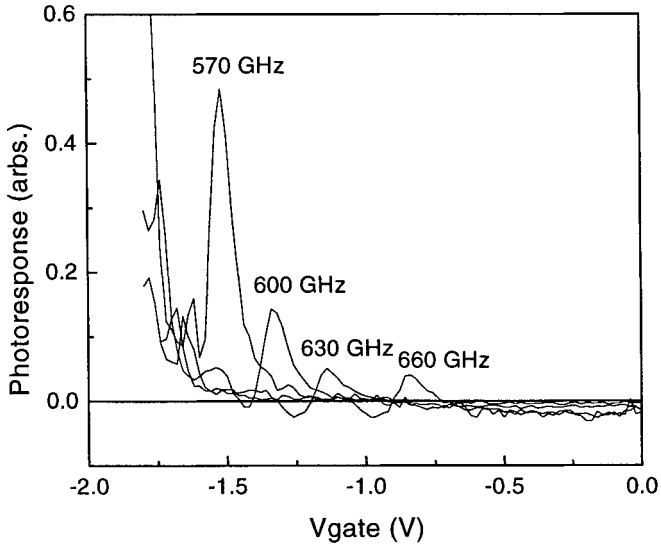

Figure 5. Terahertz photoresponse as a function of gate voltage at four different frequencies. The temperature was T=25K and the source-drain current was I_{SD}=100μA. Grating period is 4μm.

To confirm that the observed resonant response is caused by the plasmon modes underneath the grating gate, we explored another device made from the same double quantum well material and processed in the same way but with an 8 μm grating period. The lower two plots in Fig. 6 show the photoresponse at 600 GHz as a function of gate voltage at T=25K for both the 4 μm (left) and the 8 μm (right) periods.

The data for the 8 μm period grating shows a similar behavior to the 4μm grating period sample in terms of having a resonance that moves to higher electron densities as we increase the frequency, but there are several noticeable differences; a) at all frequencies the signal is basically negative, it is an increase in the conductivity of the bottom 2DEG, b) a larger number of resonances within the gate voltage range studied and c) as we bias to lower electron densities the resonances come closer together. The larger period, the greater the number of allowed standing waves in a frequency interval. For a given excitation frequency, a larger number of resonances will appear in a gate voltage range.

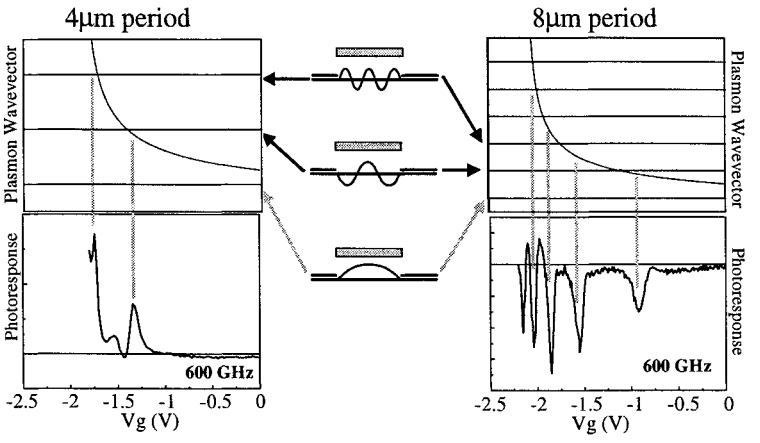

Figure 6. Top: Model plasmon wavevector as a function of gate voltage at 600 GHz. Horizontal lines correspond to wavevectors where an odd integer number of plasmon ½ wavelengths fit under the metallic part of the gate. **Bottom:** Terahertz photoresponse as a function of gate voltage at 600 GHz. **Middle column:** Schematic representation of plasmon modes underneath the metal corresponding to the observed resonances. I_{SD}=100μA and T=25K.

As further corroboration, we constructed a simple model that captures the essential physics of the problem. We modeled the collective response of the composite structure by treating the DQW as a single one, ignoring the effect of fringing fields on the ungated regions and using an equivalent circuit. In the ungated region we combine the sheet densities of the two quantum wells into one ($n_{effective} = n_{upper} + n_{lower}$) and keep it fixed. The standing waves under the grating metal are modeled by a "transmission line" with a variable density 2DEG (ranging from $n_{effective}$ to zero). The total impedance is the series combination (sum) of the impedances of the gated and ungated regions.

The upper plot in Fig. 6 helps us develop some intuition by showing the plasmon wavevector in a uniformly metallized 2DEG at a particular frequency as a function of gate voltage. The horizontal lines correspond to an odd integer number plasmon ½ wavelengths underneath the metal fingers (odd spatial harmonics). Relating the upper plot to the data we can infer that the first resonance (from right to left) corresponds to the plasmon with wavevector $3q = 3*(2\ \pi\ /a)$, the second to $5q=5*(2\ \pi\ /a)$ and so on, indicated by the parallel vertical lines where a is the period. In the middle column are schematic representations of the current density distribution under the metal gate for the corresponding resonant modes.

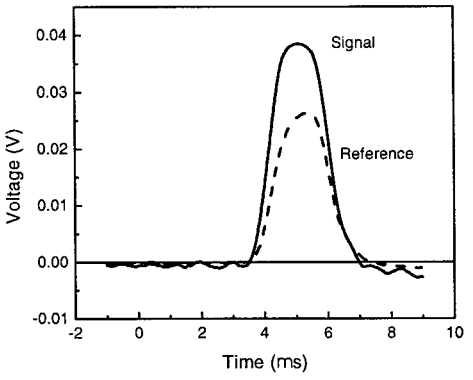

Figure 7. Time response of the double quantum well field effect transistor at resonance (solid) and the reference pyroelectric detector (dotted) for frequency = 570GHz, I_{SD}=100μA and T=25K.

Fig. 7 compares the time response of the double quantum well FET at resonance and the fast pyroelectric detector used as a reference. The frequency was 570GHz, I_{SD}=100μA and T=25K. The device is fast enough to detect the free electron lasers' rise and fall. The response time is faster than 700ns.

While it is clear that the terahertz photoconductance resonates at the standing plasmon resonance and its spatial harmonics under the grating metallization, the mechanism that produces a change in conductance is not clear. We note in Fig. 6 that the sign of the conductance change depends on the grating period. We do note that a device similar in every respect to the above but with a single quantum well displayed no resonant terahertz photoconductance; the change in conductance at resonance with the standing plasmon is conditioned on the presence of the double quantum well in the ungated part of the device. We have also observed striking dependence on in plane magnetic fields which we do not discuss here.

Discussion and Prognosis

Plasma wave detectors in a gated FET. The above results clearly demonstrate the resonant detection by the two-dimensional electron plasma confined in sub-micron field-effect transistors. The critical parameter that governs the physics of the detection problem is $\omega\tau$. We demonstrated that by increasing τ (by lowering the temperature) or increasing the detection frequency ω, one can reach a resonant detection of sub-THz radiation in a 0.15μm-gate length GaAs field effect transistor. Both the resonant and non-resonant parts of the observed photoresponse signal, as well as their evolution with temperature and frequency, were explained within the framework of a theoretical model. Theoretical estimates point to a possibility of achieving, in high mobility GaAs FETs, resonant detection up to several orders of magnitude more sensitive than that of conventional Schottky diodes[18]. There are however a number of issues that need to be addressed before such high sensitivity and tunable detectors can be realized :

- Is the submicron size compatible with requirement of the high mobility of the carriers?
- Can the limits of the device size and/or maximal frequency be changed by use of FET's based on other semiconductor heterojunctions like GaN/AlGaN or InAs/GaAlSb?
- How to incorporate efficient coupling antennas to the micron/submicron device?

Plasmon detection in grating gated double quantum well FET. We have observed a resonant photoresponse in double quantum well field effect transistors corresponding to the excitation of standing plasma waves under the metallic part of a grating gate. At the moment, we understand that the tunable resonance is caused by the composite plasma oscillations of the double quantum well structure but we do not understand the actual mechanism that gives rise to the change in conductance at resonance.

Directly related to our lack of understanding of this mechanism are other issues that need to be addressed

- What is the response time? Is it fast enough to find use as a heterodyne detector?
- As an incoherent detector it would be useful to trade responsive time for sensitivity.
- What is the projected noise equivalent power (NEP)?

From the data presented we can see that grating gated double quantum well FETs can be used as a tunable detector. An estimate of the noise equivalent power, NEP and responsivity yield $6\mu W/Hz^{1/2}$ and $R=890\mu V/W$, respectively, where we used a rough estimate of the power falling on the sample, not including terahertz losses through cryostat windows and detector coupling. These figures of merit are not competitive with good incoherent detectors. The ability to trade response time for sensitivity and NEP also needs to be addressed.

On the other hand the response time has been measured to be no slower than 700 nsec. This opens the possibility of using the device as a heterodyne detector taking advantage of electronics integrated with the detector to amplify the IF and further process the signal.

Acknowledgments

The authors would like to thank D. Enyeart and G. Ramian at the Center for Terahertz Science and Technology and W. E. Baca at Sandia National Laboratories. This work was supported by the ONR MFEL program, the DARPA/ONR THz Technology, Sensing and Satellite Communications Program and the ARO, Science and Technology of Nano/Molecular Electronics: Theory, Simulation, and Experimental Characterization. Sandia is a multiprogram laboratory operated by Sandia Corporation, a Lockheed Martin Company, for the United States Department of Energy under Contract DE-AC04-94AL85000. The work at RPI was supported by DARPA (Project Managers Drs. Edgar Martinez and Dwight Woolard) and by the National Science Foundation (Project Manager Dr. James Mink).

References

1. M. Kroug, S. Cherednichenko, H. Merkel, E. Kollberg, B. Voronov, G. Gol'tsman, H. W. Huebers, H. Richter, IEEE Transactions on Applied Superconductivity **11**, 962 (2001).
2. P. J. Burke, R. J. Schoelkopf, D. E. Prober, A. Skalare, B. S. Karasik, M. C. Gaidis, W. R. McGrath, B. Bumble, H. G. LeDuc, J. of Appl. Phys., **85**, 1644 (1999).
3. B. S. Karasik, W. R. McGrath, M. E. Gershenson, A. V. Sergeev, J. of Appl. Phys., **87**, 7586 (2000).
4. B. Bumble, H. G. LeDuc, J. A. Stern, K. G. Megerian, IEEE Transactions on Applied Superconductivity **11**, 76 (2001).
5. N. N. Iosad, V. V. Roddatis, S. N. Polyakov, A. V. Varlashkin, B. D. Jackson, P. N. Dmitriev, J. R. Gao, T. M. Klapwijk, IEEE Transactions on Applied Superconductivity, **11**, 3832 (2001).
6. See Molectron's website at www.molectron.com
7. T. W. Crow, R. J. Mattauch, R. M. Weilke, U. V. Bhapkar in Compound Semiconductor Electronics, p.209 , World Scientific Publishing, ed.by M.Shur (1996).
8. S. M. Marazita, W. L. Bishop, J. L. Hesler, K. Hui, W. E. Bowen, T. W. Crowe, IEEE Transactions on Electron Devices **47**, 1152 (2000).
9. E. E. Haller and J. W. Beeman in Proceedings of Far-IR, Sub-mm & mm Detector Technology Workshop, April 2002, Monterey, CA, in press.
10. G. E. Stillman,C. M.Wolfe, J. O. Dimmock, Solid State Comm., **7**, 5 (1969), (Proceedings of the third international conference on photoconductivity, Stanford, CA, USA, 12-25 Aug. 1969.)
11. G. Strasser, K. Bochter, M. Witzany, E. Gornik, Infrared Physics **32**, (1991).
12. M. Dyakonov and M.S.Shur in "Terahertz Sources and Systems", Kluwer Academic Publishers-Netherlands ed. by R.E.Miles, p187-207 (2001).
13. M. Dyakonov and M.S. Shur, Phys. Rev. Lett. **71**, 2465 (1993). M.Dyakonov and M.S.Shur, IEEE Trans. on Elec. Dev. **43**, 380, (1996).
14. M.Dyakonov and M.S.Shur in "Terahertz Sources and Systems" Kluwer Academic Publishers-Netherlands ed. by R.E.Miles, p187-207 (2001)
15. S. J. Allen, Jr., D. C. Tsui, and R. A. Logan, Phys. Rev. Lett., **38**, 980 (1977)
16. D. C. Tsui, E. Gornik, and R. A. Logan, Solid State Comm., **35**, 875 (1980)
17. P.J.Burke et al Appl. Phys. Lett., **76**, 745 (2000)
18. M. S. Shur and Jian-Qiang Lu, "Terahertz Sources and Detectors Using Two Dimensional Electronic Fluid in High Electron Mobility Transistors", IEEE Transactions on Microwave Theory and Techniques, **48**, 750 (2000)
19. J.-Q. Lü, M. S. Shur, J. L. Hesler, L. Sun, and R. Weikle, IEEE Electron Dev. Lett., **19** (10), 373 (1998) and J.-Q. Lu and M.S. Shur, Appl.Phys. Lett., **78**, 2587(2001)
20. W. Knap, Y. Deng, S. Rumyantsev , J.-Q. Lü, M. S. Shur, C. A. Saylor, L. C. Brunel, Appl. Phys. Lett., Vol. 80, No 18, pp. 3433-3435, May (2002) W. Knap, Y. Deng, S. Rumyantsev, and M. S. Shur, Resonant detection of subterahertz and terahertz radiation by plasma waves in submicron field effect transistors, Appl. Phys. Lett., **81**, 4637 December (2002)
21. W. Knap, V. Kachorovskii, Y. Deng, S. Rumyantsev, J.-Q. Lü, R. Gaska, M. S. Shur, G. Simin, X. Hu and M. Asif Khan, C. A. Saylor, L. C. Brunel, Journal of Applied Physics, vol. 91, No 11, 9346-9353, June (2002)
22. X. G. Peralta, S. J. Allen, M. C. Wanke, N. E. Harff, J. A. Simmons, M. P. Lilly, J. L. Reno, P. J. Burke, J. P. Eisenstein, "Terahertz photoconductivity and plasmon modes in double quantum well field effect transistors", Appl. Phys. Lett. vol. 81, No 9, pp. 1627-1629, August (2002)
23. G. E. Santoro and G. F. Giuliani, Phys. Rev. B **37**, 937 (1981).
24. S. Das Sarma and A. Madhukar, Phys. Rev. B **23**, 805 (1981).
25. D. S. Kainth, D. Richards, A. S. Bhatti, H. P. Hughes, M. Y. Simmons, E. H. Linfield, and D. A. Ritchie, Phys. Rev. B **59**, 2095 (1999).